International Research Journal of Engineering and Technology (IRJET) e-ISSN: 2395 -0056
Volume: 03 Issue: 09 | Sep-2016 www.irjet.net p-ISSN: 2395-0072

Simulation Of Welding Pool Of Metal Matrix Nanocomposites

Sasmita Kar

Resource Person, CAPGS, Biju Patnaik University Of Technolgy, Rourkela, Odisha, India

---

Abstract - *Metal Inert Gas (MIG) welding have got a lot of attention as a liquid state joining technique and provided an improved way of producing aluminum joints in a faster way. In the present work, nano Al_2O_3 particles reinforced with aluminum metal matrix nanocomposites which find applications in aircrafts are casted and MIG welded. MIG resulted in significant grain refinement and homogeneous distribution of nano alumina particles. Further simulations of the welding process of aluminium metal matrix nanocomposites (MMNCs) are studied. The analytical solution is obtained by solving a transient 3-dimensional heat conduction equation with convection and considering the boundary conditions at the surface of the weldments. The simulations have been performed with the commercial software FLUENT in ANSYS R-12 which includes moving heat sources, material deposit, metallurgy of binary aluminum, temperature dependent material properties, metal plasticity and elasticity, transient heat transfer and mechanical analyses. In order to demonstrate its usefulness in welding applications, a three-dimensional numerical simulation of the gas metal arc welding (GMAW) process using Volume of Fluid (VOF) technique has been developed based on mathematical models.*

Key words : MIG, VOF, GMAW, MMNCs, FLUENT, ANSYS R-12.

1.INTRODUCTION

Metal Matrix Composites (MMCs) reinforced with ceramic particulates offer significant performance advantages over pure metals and alloys. MMCs tailor the best properties of the two components, such as ductility and toughness of the matrix and high modulus and strength of the reinforcements. These prominent properties of these materials enable them to be potential for numerous applications such as automotive, aerospace and military industries, commercially viable to consider for industrial applications.

1.1 Background.

Particulate MMCs contain second phase particles ranging from 10 nm up to 500 μm. MMCs with a uniform dispersion of particles in the range of 10 nm–1μm are termed — Metal Matrix Nano-composites (MMNCs). With the size of reinforcement scaling down to nano scale; MMNCs exhibit more outstanding properties over MMCs and are assumed to overcome the shortcoming of MMCs such as poor ductility, low fracture toughness and machinability. It has been reported that with a small fraction of nanosized reinforcements, MMNCs could obtain comparable or even far superior mechanical MMCs can be divided into three categories: particle reinforced MMCs, short fiber reinforced MMCs and continuous fiber reinforced MMCs. Of these three categories, the fabrication cost of particulate reinforced MMCs is low, which make it attractive.

1.2 Welding.

Welding is extensively used in the construction of shipbuilding, aerospace automotive, chemical, electronic, and power generation industries. In fusion welding, parts are joined by the melting and subsequent solidification of adjacent areas of two separate parts. Safety and reliability of the welded joints depend on the weld metal geometry, composition, and structure.

Heat flow during welding is of great interest to welding engineers and metallurgists. It not only controls the size of the fusion, but also affects the properties of the resultant weld. The gas metal arc (GMA) and gas tungsten arc (GTA) welding is a process in which a coalescence of metals is produced by heating them with an arc between a metal as well as tungsten electrode and the workpiece.

The complex nature of the welding process causes difficulty in analyzing and modeling by numerical methods. These complexities include: material and thermal properties which vary with temperature,

transient heat transfer with complicated boundary conditions, moving heat sources, phase changes and transformations, complex residual stress states and the difficulties of making experimental measurements at high temperatures .In addition to these complexities, computational fluid dynamics (CFD) of the weld process must include complex thermo-fluid dynamics interactions, metallurgical transformations, material deposit, and moving heat sources.

Moving heat sources are used to generate the temperature fields during the welding process and material deposit is implemented using a variety of means. However, the global/local methodology was developed specifically to incorporate computationally intensive analyses into the design optimization program. A good quality weld is characterized by material composition, joint condition relative position of the welding arc to the joint and welding parameters such as arc current, arc voltage, and torch travel speed, etc. [81]. Therefore, choosing an appropriate set of welding parameters becomes one of the most important tasks in GTA welding process.

Due to some unrealistic assumptions, heat flow and solidification in the weld pool cannot be predicted, and poor agreement may exist between calculated and experimental results in the area immediately adjacent to the weld pool. Solving a transient three-dimensional heat conduction equation with convection boundary conditions at the surfaces of the weldment, Boo and Cho obtained the transient temperature distributions in a finite thickness plate.

Four states (solid, liquid, gas, and plasma) of several materials exist simultaneously in a small weld volume and material interactions associated with electric, magnetic, kinetic, thermal, chemical, atomic and fluidic processes take place. Aspects of the physical behavior of the cathode spots formed at the negative electrode of the welding process (for example, their retrograde motion in a transverse magnetic field and their high mobility) are still not even understood fundamentally at this time. The work described in this dissertation is aimed at establishing the usefulness of arc welding models based on accurate simulation of heat and fluid flow phenomena that incorporate empirically-calibrated material, momentum, pressure and energy inputs associated with the arc. There is considerable published literature dealing with mathematical modeling of welding arc effects on the welded material. In published literature, the spatial distributions of the direct arc heat input, the electrical current and normal pressure due to stagnation of arc plasma flow on the weld pool surface have been characterized as Gaussian density functions. Gaussian density functions are described by a single shape parameter and a total magnitude (i.e. total heat input and current) that can be obtained from experimental measurement. The plasma gas flow also exerts a shear stress on the liquid metal surface that tends to push the molten metal outward, reducing the weld penetration. The other important force due to the electric arc is Lorentz force that is induced by interaction between the current flow in the weld pool and its magnetic field. At the high welding current, the Lorentz force is dominant and largely determines the weld pool fluid flow. Other forces that induce flow in the weld pool are caused by the variation in material properties due to temperature gradients. The surface tension gradient induced flow on the weld pool surface due to the temperature gradient has major effects on weld pool shape. The final weld shape can be significantly changed by the contents of the surface active elements (e.g. sulfur) that alter the direction of surface tension gradient induced flow (Marangoni flow). The high sulfur steel tends to generate the inward fluid flow pattern that tends to produce the deeper penetration, and the outward fluid flow pattern that generates the shallow penetration is expected for the low sulfur steel. Change of density with temperature also induces buoyancy forces that stir the weld pool. Even these relatively well-understood flow-inducing forces are related to temperature gradients caused by welding heat, mass and momentum inputs. Thus, prediction of even these relies on accurate modeling the arc inputs. The other work described in this dissertation based on the numerical simulation of

arc welding process is that ability to predict the deposition of filler metal droplets, the shape of the free surface of the weld pool and solidified weld metal will be useful to welding engineers. In this regard, it is noted that there are several critical weld defects that are related to weld shape. The formation of weld bead humps is a defect mode that sets an upper limit on the arc welding travel speed. The shape of the wetting contact line between weld metal and adjacent un-melted base material is fundamental to prediction of lack of fusion defects and usually determines the fatigue strength of welds. The arc welding simulation is useful to use the numerical simulation as a key tool for the investigation of the welding defect such as hump formation at the high travel speed weld and the process development to eliminate the welding defect based on the understanding of its mechanism. Another capability of using the numerical simulation is its flexibility of studying the phenomenon under varying conditions (e.g. welding par

ameters, thermal mechanical properties etc), which are very difficult to acquire experimentally.

2.EXPERIMENT

The nanocomposites are prepared by Padhi et al which is subjected to welding. The experimental setup for preparation of Al & Al_2O_3 MMNCs.. In the experiment, MMNCs nanocomposites plates were used as the workpieces to be welded with gas tungsten arc welding machine under various welding conditions. Detailed compositions and weight percentages of 5456 aluminum plates are shown in Table 5.1. The welded plates are 2 mm thick, 200 mm wide and 250 mm long whose figure is shown in Figure 5.3. The TEM microstructures of nano composites was shown in another Figure. In addition, the experimental conditions and thermal properties of the welded plates were the same as those used in the numerical calculation and were shown in Table 5.2. The physical properties used in the calculations are fixed as the values at 300°C, which is approximately the average value of room temperature and melting temperature.

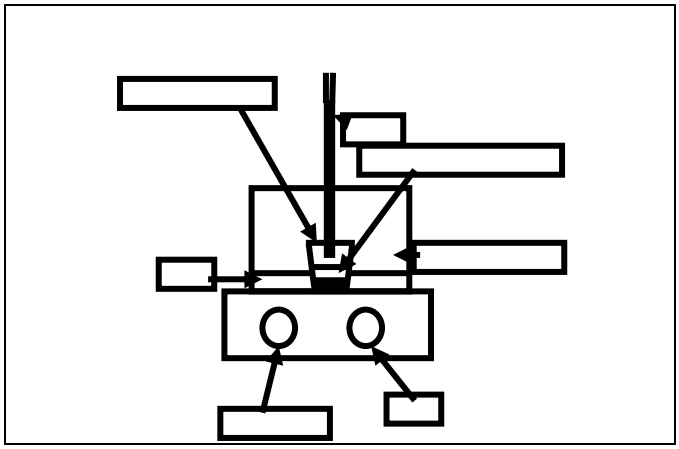

Figure 5.1 : Experimental setup for preparation of Al & Al_2O_3 MMNCs

Table 5.1: Composition of MMNCs for welding

Sh no	Material	Weight %
1	Commercially pure aluminium	98.5
2	Calcined alumina (AL_2O_3)	1.5

Also, note that the effective liquid conductivity is about 1.5 times the value of the solid thermal conductivity whereas the specific heat of liquid aluminum is equivalent to that of solid one. The GTA welding parameters were welding voltage: 10 V, welding current: 86A-125A, travel speed: 3 mm/sec-7.24 mm/sec, respectively. Oxide films were polished off the surfaces of the plates before the experiment. The polished surface was then cleansed with acetone just before welding. Furthermore, the workpieces were thermally insulated from the fixtures in order to avoid heat sinks during welding. Argon gas was used for both welding and protecting the underside of the plate. Twelve K-type thermocouples were positioned in the workpieces as shown in Figure 5.3, six on the top and six on the bottom surfaces of the aluminum plates. All the thermocouples were precalibrated by a quartz thermometer with 0.1°C precision, and all of the data signals were collected and converted by a data-acquisition system (a hybrid recorder). The data-acquisition system then transmitted the converted signals through a general purpose interface bus to the host computer for further operation. The experiments were repeated under

varying process variables such as arc current, travel speed and initial temperature of the welded plates. The detail experimental results, i.e. heat affected zone (HAZ) are shown in the figure.

Figure 5.2: Experimental set up

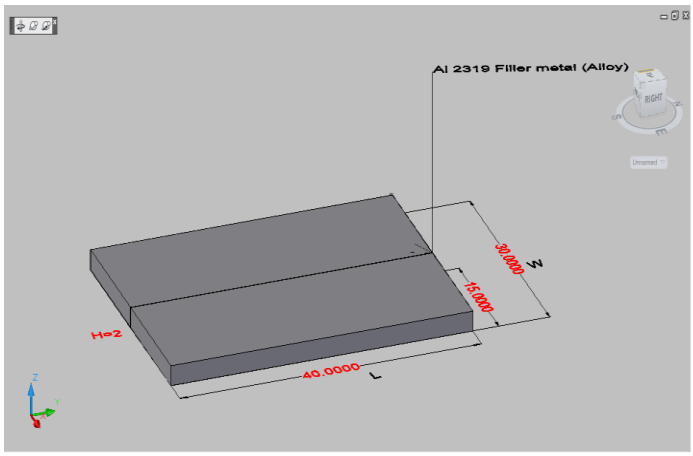

Figure 5.3: Schematic diagram of MMNCs plates

Table 5.2: Thermal properties of composites

3.RESULTS AND DISCUSSIONS

The input data for simulation parameters determined from direct measurements and from the literature. The MMNCs GMA welding was conducted, and simulation results were validated with experimental results.

3.1 MICROSTRUCTURE COMPARISON.

The optical micrographs of the welded section of MMNCs at different sections are shown in Figure. In this samples are taken at two different places and polished and optical microstructures are taken. It is seen from both the micrograph the welding structure at the center of weld pool is net worked structure and just adjacent to the weld pool it is less networked. This is because of the solidification process of weld pool. At the weld pool the solidification takes later compared to the side.

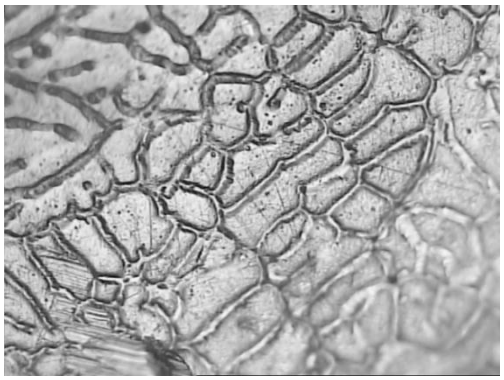

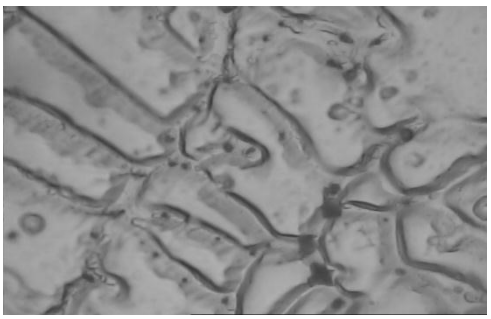

Figure : Optical micrographs of two different sections of welded joints

The HRTEM microstructure of the welded pool is shown in the Figure 5.3. Here the nano particles are not visible. This may because of agglomeration of the particles at certain point which is not observed.

3.2 WELD GEOMETRY COMPARISONS.

Temperature in ^{0}K	Thermal conductivity wm-k	emissivity
300	143	0.05
400	151	0.12
500	159	0.17
600	167	0.2
700	169	0.21
800	173	0.23
900	179	0.25

A very common way to validate weld simulations is to compare the dimensions of weld cross-sections measured from experiments with those predicted by the simulation.

Figure shows the SEM microstructure of weld pool structure where the nanoparticles are distributed prominently. It seems that during welding the distributions of particle is not getting affected. This is because of the size effect.

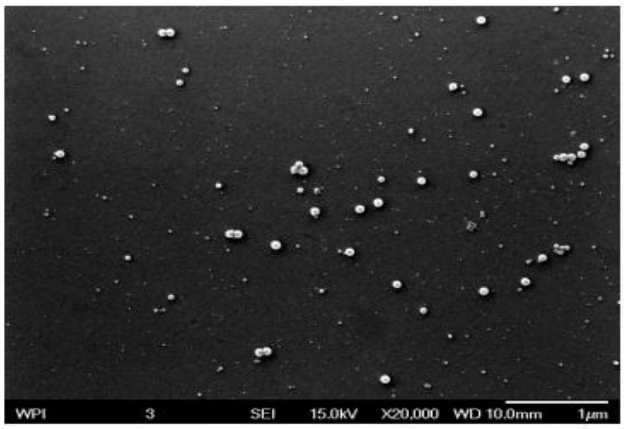

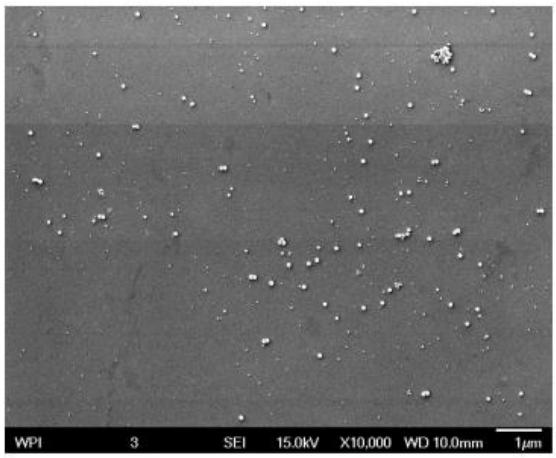

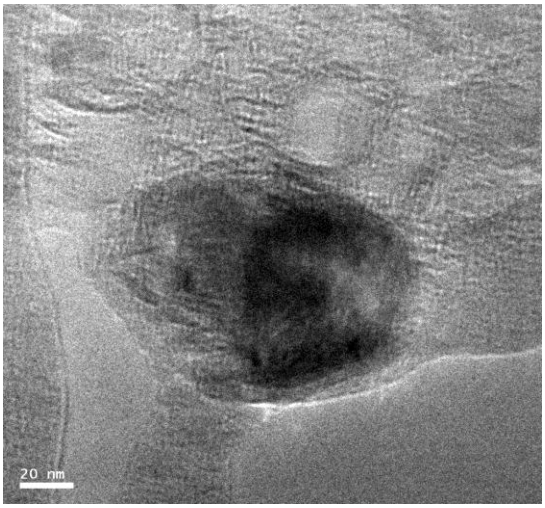

The HRTEM microstructure of the welded pool is shown in the Figure. Here the nano particles are not visible. This may because of agglomeration of the particles at certain point which is not observed.

3.3 WELD GEOMETRY COMPARISONS.

A very common way to validate weld simulations is to compare the dimensions of weld cross-sections measured from experiments with those predicted by the simulation. In Figure, the actual weld cross-sectional images and the simulated cross-sectional weld views are displayed in order to compare reinforcement, radius, toe angles, and penetration.

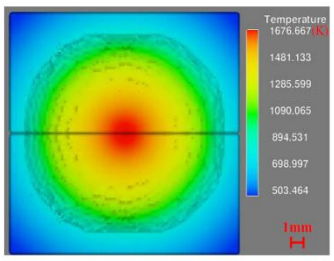

The quantitative comparison of the simulation and the experimental results is given in Table 6.1. Weld reinforcement measurements of the actual weld shown in Figure above vary from 1.9 mm to 2.3 mm depending on the measuring locations (A and B). The average height, 2.1 mm, is comparable to the simulated weld height of 1.88 mm. There are two penetrations observed at the center and the edge of the weld shown in Figure. The inward circulation developed by drop momentum, arc pressure and Lorentz force generates the center weld penetration, but the outward circulation induced by Marangoni force and plasma drag force produces the penetration at the weld edge.

Table 6.1: Temperature field comparision at different position of the weld

Particulars	Center position of the weld (temp)	Left	Right	Top	Bottom
Actual	1650	1032	1020	1030	1025
Simulated	1681	1100	1100	1100	1100
Error	-1.88%	-6.59%	-7.84%	-6.79%	-7.32%

To compare weld penetrations, the simulation result at the weld termination time (1.8 s) when the maximum penetration occurs during the weld was used to measure the weld penetrations, and two clear circulations observed. In summary,

differences in weld radius, the height of weld reinforcement, weld toe angles, and penetration at the edge are 10 percent, but the simulated weld penetration at the center is significantly deeper than the experimental measurement. This discrepancy is attributed to the high efficiency of drop momentum transfer and heat transfer mainly due to fluid convection in the simulation. According to Figure, metal transfer images show that molten droplets at the initial weld time up to 0.5 sec were not spherical and also the location of droplet impingement on the weld pool was somewhat random during the weld. Therefore, at the initial weld time before 0.5sec, the experimental weld pool was not yet as developed as the simulated one and the weld metal convection that effectively transfers momentum and heat to the bottom of the weld pool was not as strong.

4.CONCLUSION

Numerical and experimental studies of the welding parameters on the plates of MMNCs were carried out by metal inert gas arc welding processes. Major conclusions of this study are summarized as follows:

VOF technique was used to implement a simulation of stationary P-GMA welding that included non-isothermal free-surface fluid flow. Buoyancy, Marangoni, arc pressure, drag, and Lorenz forces were mathematically modeled and implemented in the numerical simulation.

P-GMA arc size and droplet transfer were measured from arc images and used to determine some simulation variables. Direct comparisons of predicted and measured weld geometry, time-varying deposit radius curve, and temperature history from thermocouple measurement were used to validate the P-GMA stationary welding simulation. The simulation predicted deeper weld penetration than those measured experimentally, a difference that was attributed to consistent droplet impact location in the simulation versus random droplet impact in the experiments.

Simulation tests with individual changes of variables (Gaussian heat distribution, Gaussian current distribution, total force, and Gaussian pressure distribution) provided insight into the effects of these variables on fluid flow patterns and weld penetration. The large heat distribution with a fixed total heat input decreased the weld penetration, the constricted current density distribution drastically increased the weld penetration but decreased the weld radius, and the reduced total force and the large arc pressure distribution radius decreased the weld penetration.

5.REFERENCES

1. Greenwood, G. W., and Johnson, R. H., 1965, "The Deformation of Metals Under Small Stresses During Phase Transformations", *Proceedings of the Royal Society of London. Series A, Mathematical and Physical Sciences,* , pp. 403-422.
2. G.K.Hicken and C.E.Jackson: Effects of Applied Magnetic Fields on welding Arcs, Welding Journal, Vlo.45, No.8, 513s-518s, 1966.
3. Malvern, L. E., 1969, *Introduction to the Mechanics of a Continuous Medium*, Prentice-Hall, Inc., Englewood Cliffs, NJ, pp. 233, 338.
4. Martin, J. B., 1975, *Plasticity: Fundamentals and General Results*, The MIT Press, Cambridge, MA, pp. 63-65.
5. K.Masubuchi, Analysis of welded structures: Residual stresses, Distortion and Their Consequences, Pergamon Press, Oxford,1980.
6. Masubuchi, K., 1980, *Analysis of Welded Structures-Residual Stresses, Distortion, and Their Consequences,* Pergamon Press, New York, NY, pp. 205.
7. M.L.Lin: Transport Phenomena in Material Processing, ASME-PED, No.10, 63-69, 1983.
8. Dubois, D., Devaux, J., and Leblond, J. B.,1984, "Numerical Simulation of a Welding Operation: Calculation of Residual Stresses and Hydrogen Diffusion," ASME *Fifth International Conference on Pressure Vessel Technology, Materials and Manufacturing*, **II,** San Francisco, CA, pp. 1210 - 1238.
9. Hatch, J. E., 1984, *Aluminum: Properties and Physical Metallurgy*, American Society for Metals, Metals Park, OH, pp. 42.
10. G.M.Oreper and J.Szekely: Heating and Fluid-flow Phenomena in Weld Pool, J. Fluid Mech., Vol.147, part I, 53-79, 1984.

11. Goldak, J., Chakravarti, A., and Bibby, M., 1984, "A New Finite Element Model for Welding Heat Sources," *Metallurgical Transactions B*, **15B**, pp. 299-305.
12. Chen Chu: numerical analysis application in welding, Publishing Company of Shanghai Jiaotong University, 230, 1985.
13. Karlsson L. Thermal stresses in welding. In: Hetnarski RB, editor. Thermal stresses I. Elsevier Science Publishers; 1986. p. 299–389.
14. Leblond, J. B., Mottet, G., and Devaux, J. C., 1986, "A Theoretical and Numerical Approach to the Plastic Behaviour of Steels During Phase Transformations - I. Derivation of General Relations", *J. Mech. Phys. Solids*, **34**, pp. 395-409.
15. Leblond, J. B., Mottet, G., and Devaux, J. C., 1986, "A Theoretical and Numerical Approach to the Plastic Behaviour of Steels During Phase Transformations - II. Study of Classical Plasticity for Ideal-Plastic Phases", *J. Mech. Phys. Solids*, **34**, pp. 411-432.
16. Beck, G., Denis, S., and Simon, A., 1988, "The Influence of Thermomechanical Treatment on Residual Elastic Microstrain in an Aluminium Alloy", *2nd International Conference on Residual Stresses*, Nancy, France, pp. 765-770.
17. Wyss, R. K., and Sanders, Jr., R. E., 1988, "Microstructure-Property Relationship in a 2XXX Aluminum Alloy with Mg Addition", *Metallurgical Transactions A*, **19A**, pp. 2523-2530
18. Oddy, A. S., Goldak, J.A., and McDill, J. M. J., 1989, "Transformation Plasticity and Residual Stresses in fSingle-Pass Repair Welds," ASME *PVP- Weld Residual Stresses and Plastic Deformation*, **173**, pp. 13-18.
19. Karlsson, L., Jonsson, M., Lindgren, L. E., Nasstrom, M., and Troive, L., 1989, "Residual Stresses and Deformations in a Welded Thin-walled Pipe," ASME *PVP-Weld Residual Stress andPlastic Deformation*, , pp. 7-10.
20. Boyles, L.G., 1989, "Computer Analysis of Failure Modes in Welded Joints," ASME *PVPWeld Residual Stress and Plastic Deformation*, **173**, pp. 1-4.**173**
21. Boyles, L.G., 1989, "Computer Analysis of Failure Modes in Welded Joints," ASME *PVPWeld Residual Stress and Plastic Deformation*, **173**, pp. 1-4.**173**
22. Thiery, J., Archambault, P., and Moreaux, F., 1989, "Influence of a Traction Stress on the Hardening Kinetics of Aluminium Alloys", *2nd International Conference on Residual Stresses*, Nancy, France, pp. 771-776.
23. Karlsson, R.I., and Josefson, B.L., 1990, "Three-Dimensional Finite Element Analysis of Temperatures and Stresses in a Single-Pass Butt-Welded Pipe," ASME *Journal of Pressure VesselTechnology*, **112**, pp. 76-84.
24. Oddy, A. S., McDill, J. M. J., and Goldak, J. A., 1990, "Consistent Strain Fields in 3D FiniteElement Analysis of Welds," ASME *Journal of Pressure Vessel Technology, Technical Briefs*,, pp. 309-311.
25. J.C. Villafuerte, H.W. Kerr: Electromagnetic stirring and Grain Refinement in Stainless Steel GTA Welds, Welding Research Supplement, 1s-13s, 1990.
26. M. Malinowski-Brodnicka, G. den ouden: Effect of Electromagnetic Stirring on GTA Welds in Austenitic Stainless Steel, Welding Research Supplement, 52s-59s, 1990
27. Wu Chuansun: Numerical analysis of welding thermal process, Publishing company of Harbin Industry University, 116-118,1990